Cerebral hemodynamics in arteriovenous malformations: evaluation by single-photon emission CT.

S Takeuchi, H Kikuchi, J Karasawa, Y Naruo, K Hashimoto, T Nishimura, T Kozuka and M Hayashi

AJNR Am J Neuroradiol 1987, 8 (2) 193-197
http://www.ajnr.org/content/8/2/193

Cerebral Hemodynamics in Arteriovenous Malformations: Evaluation by Single-Photon Emission CT

Shigekazu Takeuchi[1]
Haruhiko Kikuchi[1]
Jun Karasawa[1]
Yoshito Naruo[1]
Kenji Hashimoto[1]
Tsunehiko Nishimura[2]
Takahiro Kozuka[2]
Makoto Hayashi[2]

Cerebral hemodynamics in six patients with supratentorial arteriovenous malformations (AVMs) were studied by using single-photon emission CT with three types of radioactive isotopes: N-isopropyl-p-[^{123}I] iodoamphetamine, ^{81m}Kr, and ^{99m}Tc-RBC in order to determine the local cerebral blood flow and blood volume associated with these malformations. The AVMs were shown to have high flow while other areas of the brain, including the contralateral hemisphere, had variable areas of diminished perfusion. There was increased blood volume in the regions of AVMs, and poor but evenly distributed blood volume in the other regions. CO_2 reactivity during hypocapnia was preserved throughout the brain except for the region of the AVMs. In large AVMs, the ischemic state surrounding the nidus was considered to be caused mainly by the cerebral steal phenomenon.

Cerebral arteriovenous malformations (AVMs) are unique structural anomalies that consist of clusters of vessels with free communication between the arterial and venous systems without an interposed capillary bed. Pulsatile compression of the surrounding brain tissue by the AVM itself, intracranial hemorrhage, hydrocephalus, and the cerebral steal phenomenon may contribute to neurologic deficits. The introduction of microsurgical techniques has reduced the risk of neurosurgical sequelae associated with excision of cerebral AVMs and has extended the indication for surgical treatment. In many of the patients with large or deep-seated AVMs, however, total excision is difficult to perform. Nonsurgical medical care, incomplete ligation of the feeders, and embolization procedures are the only treatments in these patients.

Cerebral hemodynamics in patients with cerebral AVMs have been studied by various methods before, during, and after surgery; however, most of these methods have been studies of total cerebral blood flow [1, 2] or two-dimensional techniques such as intracarotid injection of ^{85}Kr or ^{133}Xe [3], ^{133}Xe inhalation [4], and IV injection of ^{133}Xe [5]. Hemodynamic study using three-dimensional methods such as emission tomography and stable xenon-enhanced CT has rarely been reported [6]. It is controversial whether or not there is an ischemic zone surrounding AVMs without a hemorrhagic history. We studied cerebral hemodynamics in patients with AVMs using single-photon emission CT (SPECT) with three types of radioactive isotopes: N-isopropyl-p-[^{123}I] iodoamphetamine, ^{81m}Kr, and ^{99m}Tc-RBC in order to determine local blood flow and blood volume in the regions of the AVMs and surrounding cerebral tissue.

Materials and Methods

Six patients with supratentorial AVMs were studied. They were 9–49 years old (average age, 29). SPECT studies were performed in three patients in whom the intracranial hemorrhage was more than 1 month old. Clinical and CT data are summarized in Table 1.

SPECT images were obtained by using a rotating gamma camera with dual heads PHO/

Received August 1, 1985; accepted after revision August 26, 1986.

[1] Department of Neurosurgery, National Cardiovascular Center, Osaka 565, Japan. Address reprint requests to S. Takeuchi, Department of Neurosurgery, Brain Research Institute, Niigata University, Asahimachi 1, Niigata 951, Japan.

[2] Department of Radiology, National Cardiovascular Center, Osaka 565, Japan.

AJNR 8:193–197, March/April 1987
0195–6108/87/0802-0193

TABLE 1: Summary of Clinical and CT Findings in Patients with AVMs

Case No.	Age	AVM		Clinical Manifestations	Hemorrhage	CT
		Site	Size			
1	19	L basal ganglia	Large	R hemiparesis	—	Calcification
2	22	L frontal lobe, basal ganglia	Large	Convulsion, apraxia, transient aphasia	—	Slight mass effect
3	9	R basal ganglia	Moderate	L hemiparesis	ICH, IVH	Small LDA
4	49	L basal ganglia	Moderate	Transient unconsciousness, R hemiparesis	SAH	Small LDA
5	41	L parietal lobe	Small	Convulsion	—	No abnormal finding
6	35	L temporal lobe	Small	R homonymous hemianopsia, aphasia	ICH	Moderate LDA

Note.—L = left; R = right; ICH = intracerebral hemorrhage; IVH = intraventricular hemorrhage; SAH = subarachnoid hemorrhage; LDA = low-density area.

GAMMA LFOV-E and the Scintipac 2400 computer system (Shimazu Co., Japan). The radioactive isotopes were N-isopropyl-p-[^{123}I] iodoamphetamine (IMP) and ^{81m}Kr (Kr) (Nihon Mediphysics Co., Japan) for local cerebral blood flow and ^{99m}Tc-RBC (Tc) (Daiichi Radioisotope Institute Co., Japan) for local cerebral blood volume. The double gamma cameras were rotated 18 times at discrete and equal angles in increments of 10°. Data acquisition time at only one angle was 30 sec in four patients and 1 min in two patients in SPECT-IMP and 10 sec in SPECT-Kr and SPECT-Tc in all the patients. To further improve the results obtained by averaging opposed projection data, a correction for attenuation was performed in SPECT-IMP and SPECT-Tc using a linear attenuation coefficient. In the Kr study, however, no correction for attenuation was needed. In SPECT-IMP, data acquisition was started 30 min after the IV injection of IMP (3 mCi [111 MBq] of ^{123}I); the sampling time was about 10 min in four patients and about 20 min in two patients [7]. Correction for attenuation was performed using a 0.12 linear attenuation coefficient. In SPECT-Kr, data acquisition was obtained for about 4 min during the continuous infusion of ^{81m}Kr (10–15 mCi [370–555 MBq]/min) into the ascending aorta by the transfemoral catheter technique [8, 9]. In the Kr study, equilibrium images during the continuous arterial infusion were required because of the 13-sec half-life of ^{81m}Kr [10]. In SPECT-Tc, in vivo RBC labeling was done with two consecutive IV injections, first of Sn-pyrophosphate and then of ^{99m}Tc-pertechnetate (15 mCi [555 MBq]) at an interval of about 30 min between the two injections in order to obtain a high labeling rate [10]. Data acquisition time was about 4 min, and correction for attenuation was performed using 0.12 of the linear attenuation coefficient.

Results

The clinical manifestations included were hemiparesis, convulsion, aphasia, apraxia, transient loss of consciousness, and homonymous hemianopsia. In two patients (cases 1 and 2), the clinical symptoms and signs slowly progressed without intracranial hemorrhage. Intracranial hemorrhage was encountered once in three patients (cases 3, 4, and 6). In these three patients, neurologic deficits were caused by hemorrhages. There were neither high-density lesions nor mass effect due to a hematoma in X-ray CT findings at the time of the SPECT studies. The sites of AVMs were the basal ganglia in three patients (cases 1, 3, and 4); the cerebral cortex in two patients (cases 5 and 6); and the cerebral cortex, subcortex, and basal ganglia in one patient (case 2). The sizes of the AVMs were not measured on the angiograms because digital subtraction angiography was performed with varying magnifications in most of the examinations. However, the sizes were classified into three types from CT findings after contrast infusion. Two patients each had AVMs of large, moderate, and small sizes. In two patients (cases 1 and 3), the AVM was filled on ipsilateral carotid and vertebral angiograms. There was visible filling of the AVMs via the anterior communicating artery on contralateral carotid angiograms in two patients (cases 1 and 2) and faint filling in one patient (case 4). In the other two patients (cases 5 and 6), the AVM was seen only on ipsilateral carotid angiography. Precontrast CT findings showed calcification in the nidus of the AVM in one patient (case 1), slight compression of the lateral ventricle due to the AVM in one patient (case 2), and small and moderate low-density lesions in two (cases 3 and 4) and one (case 6) patients, respectively.

In SPECT-IMP, the regions of the nidus were seen as decreased activity in all patients (case 1, Fig. 1). The adjacent zones were also shown as slightly decreased activity and were observed mainly in watershed areas. In the patient with the large nidus and high-flow shunt, decreased activity on SPECT-IMP was also found in the contralateral hemisphere (case 1, Fig. 1). In this patient, a carotid angiogram on the contralateral side showed the AVM filling through the anterior communicating artery.

In SPECT-Kr, the regions of the nidus were shown as increased activity (case 1, Fig. 1; case 6, Fig. 2). Decreased activity was seen in the surrounding regions, especially in the watershed areas. This surrounding decreased activity was observed more extensively and severely in SPECT-Kr than in SPECT-IMP. In four patients with large- or moderate-sized nidus, decreased activity was observed even in the contralateral hemisphere (case 1, Fig. 1). During hypocapnia due to hyperventilation, radioactive counts were reduced in other areas except for the regions of the nidus (case 1, Fig. 3). Thus, radioactive counts in the region of the nidus were relatively increased and seemed to be enlarged.

In SPECT-Tc, the regions of the nidus were found as increased activity in all four patients. The increased activity was also shown in the regions of the draining veins in two patients with large draining veins (case 1, Fig. 1). Radioactive counts in other areas except for the nidus were almost evenly distributed.

The SPECT images are summarized in Table 2.

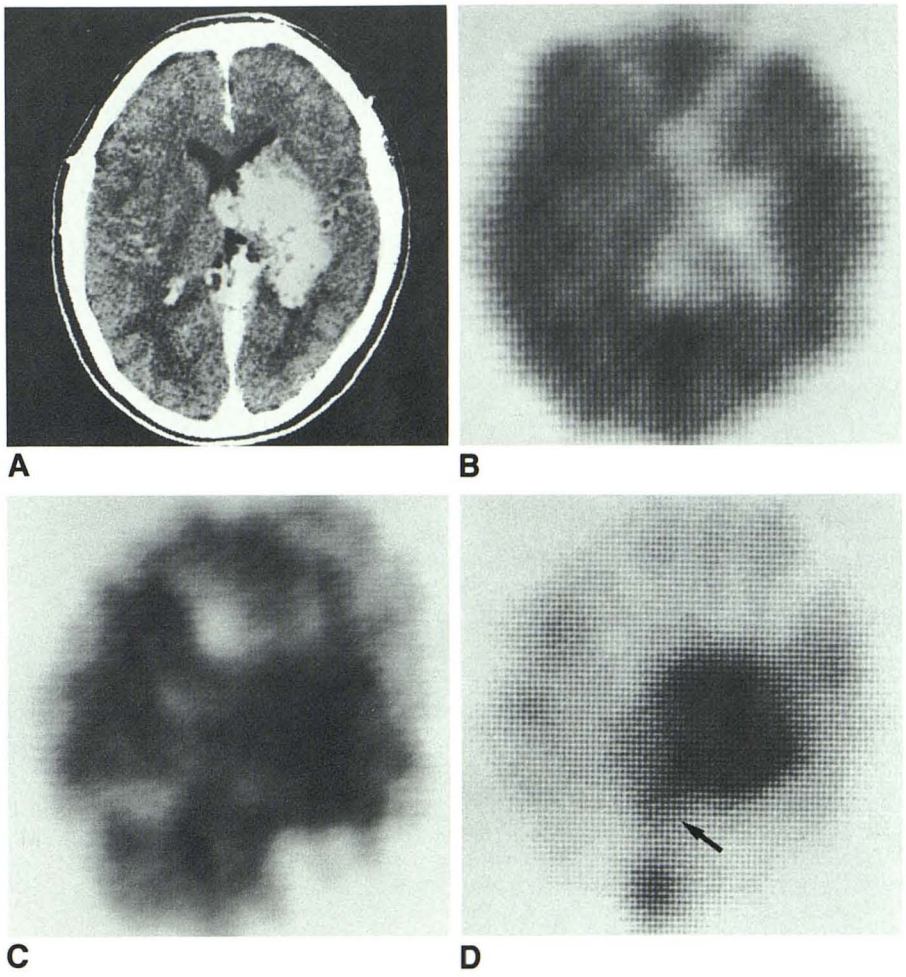

Fig. 1.—Case 1.
A, Postinfusion CT scan. Large AVM in region of basal ganglia.
B, SPECT-IMP. Low activity in nidus of AVM, in bifrontal watershed areas, and in left temporoparietal region.
C, SPECT-Kr. Increased and decreased activity in nidus of AVM and in surrounding zones including contralateral hemisphere.
D, SPECT-Tc. Nidus and draining veins (*arrow*) are seen as increased activity, but radioactivity of other regions is even.

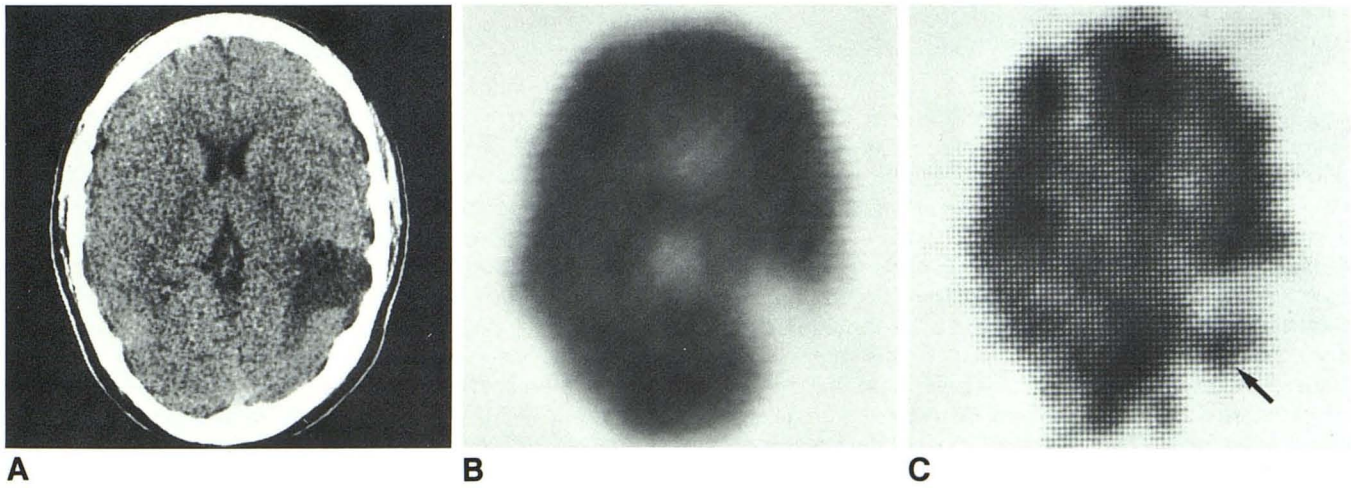

Fig. 2.—Case 6.
A, Unenhanced CT scan. Low-density lesion is in posterotemporal region on left side.
B, SPECT-IMP. Low activity is in left posterotemporal region.
C, SPECT-Kr. Nidus of AVM is seen as increased activity (*arrow*) in larger area of decreased activity.

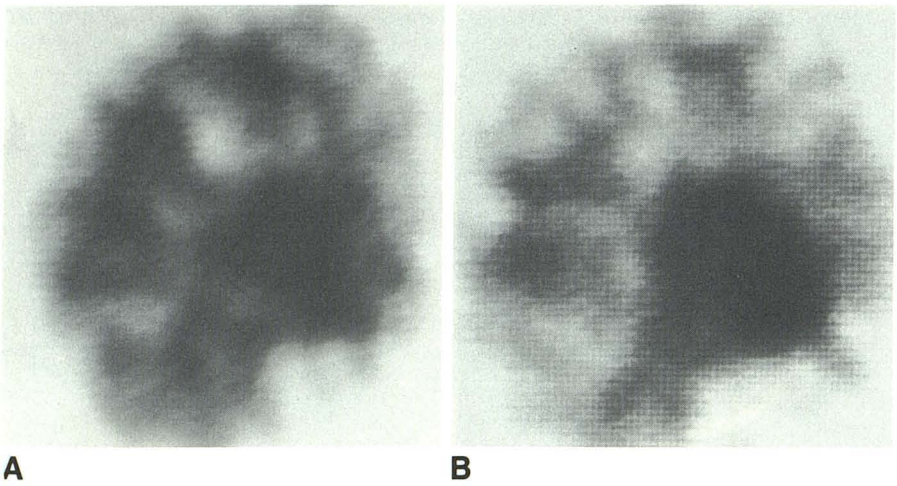

Fig. 3.—Case 1. SPECT-Kr.
***A*, At rest ($PaCO_2$: 34.4 mm Hg).**
***B*, Hypocapnia due to hyperventilation ($PaCO_2$: 21.7 mm Hg). Radioactive counts are reduced during hypocapnia in other regions except for region of nidus.**

TABLE 2: Summary of Single-Photon Emission CT (SPECT) Images in Patients with AVMs

No.	Size of AVM	Hemorrhage	LDA on CT	SPECT-IMP		SPECT-Kr			SPECT-Tc	
				Nidus	Surrounding	Nidus	Surrounding	HV	Nidus	Surrounding
1	Large	−	−	Decreased activity	Decreased activity[a]	Increased activity	Decreased activity[a]	+	Increased activity[b]	NAF
2	Large	−	−	Decreased activity	Decreased activity	Increased activity	Decreased activity[a]	+	Increased activity[b]	NAF
3	Moderate	+	+	Decreased activity	Decreased activity	Increased activity	Decreased activity[a]	+	Increased activity	NAF
4	Moderate	+	+	Decreased activity	Decreased activity	Increased activity	Decreased activity[a]	+	Increased activity	NAF
5	Small	−	−	Decreased activity	Slightly decreased activity	Increased activity	Decreased activity	+	NP	NP
6	Small	+	+	Decreased activity	Decreased activity	Increased activity	Decreased activity	NP	NP	NP

Note.—AVM = arteriovenous malformation; LDA = low-density area; HV = response of surrounding zone by hyperventilation; NAF = no abnormal findings; NP = not performed.

[a] Includes decreased activity in contralateral hemisphere.

[b] Includes increased activity of drainage vein.

Discussion

In the study of the hemodynamics of cerebral AVMs, the intravascular flow of the nidus must be distinguished from the surrounding tissue flow. It is controversial as to whether the blood flow in the adjacent zones to the nidus is decreased and if so why the flow in these zones is decreased. The purpose of our study was to define tissue flow, intravascular flow, and cerebral blood volume in brains with AVMs by using three types of radioisotopes and to estimate the cerebral steal phenomenon.

The initial distribution of IMP is useful for imaging relative regional brain perfusion because first-pass extraction efficiency in the brain is high, washout is slow, brain-blood ratios are high, and the physical properties of ^{123}I (T1/2 = 13 hr, 159 keV photon) are favorable for scanning [11, 12]. High levels of brain activity are maintained for several hours. The quantitative initial single-pass clearance of the agent in the brain suggests its usefulness in evaluating regional brain perfusion. Therefore, SPECT-IMP images are considered to show the mapping of local cerebral tissue flow [13]. In the Kr study, under continuous intraaortic infusion of a solution of ^{81m}Kr (T1/2 = 13 sec; produced from its parent, 4.6 hr ^{81}Rb), this tracer will never reach equilibrium within the brain because of the rapid radioactive decay. Therefore, its distribution will reflect regional arrival of the nuclide, indicating regional cerebral blood flow rather than volume [14].

Cerebral blood flow studies using the inert gas diffusion techniques of Shenkin et al. [1] and Lassen and Munck [2] only show large shunt flow. High flows characteristic of AVMs are also noted in the intracarotid injection method of radioactive krypton-85 [3] and the xenon-133 inhalation method [4]. In our SPECT-IMP studies, the regions of the nidus were observed as decreased activity in all the patients. On the other hand, in SPECT-Kr, increased activity was found in the region of the nidus, even in the low-density lesions seen with CT. On the basis of our findings, we believe there is intravascular high perfusion with little tissue flow in the region of the nidus. It seems likely that previous reports [1–4] reveal only intravascular high flow in the AVMs. Decreased cerebral

tissue flow in brains with AVMs were not shown by these previous methods.

In both SPECT-IMP and SPECT-Kr, the zones adjacent to the nidus are also seen as decreased activity with their sizes varying from patient to patient. This diminished activity is more profound in SPECT-Kr than in SPECT-IMP and is present regardless of a history of intracranial hemorrhage. Since low perfusion is found in many areas without intracranial hemorrhage (cases 1, 2, and 5) where there are areas of no low attenuation on X-ray CT findings, we believe that most of the low-perfusion areas are caused by cerebral ischemia. Besides the ipsilateral hemisphere, the low-perfusion areas are shown even in the contralateral hemisphere in patients with high-flow shunts (see Fig. 1).

The ischemic state surrounding AVMs has been thought to be caused either by bleeding around the AVM causing compression of the surrounding tissue, vasospasms, cerebral edema, hydrocephalus, massive overload of the venous return [15], or by stealing of blood flow into the AVM [16]. Yamada [5] measured regional cerebral blood flow in patients with AVMs by the IV injection method of xenon-133. The preoperative regional cerebral blood flow on the side of the AVM was markedly decreased while that of the contralateral hemisphere was less affected. He believed that a low value of regional cerebral blood flow was related to ischemia secondary to compression from a hemorrhage rather than to a cerebral steal [16] because of the high rate of recent bleeding in his cases. Yamada also reported that the postoperative improvement in cerebral blood flow, not only in the AVM site but also in the contralateral hemisphere, corresponded to the patient's general condition of mental and physical improvement. On the other hand, Okabe et al. [6] measured cerebral blood flow with xenon-enhanced CT. Their results indicated that local cerebral blood flow values were significantly reduced in both hemispheres, especially in regions surrounding the AVM, and these observations lent objective support to previous speculations of cerebral ischemia caused by steal [16]. Previous authors thought that progressive and/or fluctuating deficits in neurologic and mental status were indeed based on cerebral steal. In our study, two patients with large AVMs showed progressive neurologic deficits without intracranial hemorrhage. We believe also that the ischemic changes in the areas surrounding AVMs were due to a cerebral steal phenomenon.

In the blood-volume study by SPECT-Tc, increased volume was shown in the region of the AVM along with the large draining veins. Neither irregularity nor asymmetry of the blood volume was identified in regions other than the nidus and the draining veins, despite the irregular distribution of the blood flow.

In SPECT-Kr, radioactivity during hypocapnia was reduced in areas other than the nidus because of hyperventilation. Thus, we believe as others do [17] that CO_2 reactivity is preserved in regions other than the AVM nidus during hypocapnia.

Cerebral ischemia was confirmed in brains with AVMs in our SPECT study and was thought to be caused by the cerebral steal phenomenon, especially with large AVMs. In the ischemic regions of the brain with these large AVMs, normo- or hyperperfusion might occur immediately after ligation or embolization procedures of the feeders to the AVM when there is normal systemic arterial pressure [18]. The direct increase of perfusion may cause the cerebral edema and even the cerebral hemorrhage [19, 20]. To prevent these unfavorable events, embolization or ligation of the feeders should be performed in a stepwise manner, and barbiturate protection or controlled hypotension should be undertaken [20].

REFERENCES

1. Shenkin HA, Spitz EB, Grant FC, Kety SS. Physiological studies of arteriovenous anomalies of the brain. *J Neurosurg* **1948**;5:165–172
2. Lassen NA, Munck O. Cerebral blood flow in arteriovenous anomalies of the brain determined by the use of radioactive krypton 85. *Acta Psychiatr Scand* **1956**;31:71–80
3. Häggendal E, Ingvar DH, Lassen NA, et al. Pre- and postoperative measurements of regional cerebral blood flow in three cases of intracranial arteriovenous aneurysms. *J Neurosurg* **1965**;22:1–6
4. Menon D, Weir B. Evaluation of cerebral blood flow in arteriovenous malformations by the xenon 133 inhalation method. *Can J Neurol Sci* **1979**;6:411–416
5. Yamada S. Arteriovenous malformations in the functional area: surgical treatment and regional cerebral blood flow. *Neurol Res* **1982**;4:283–322
6. Okabe T, Meyer JS, Okayasu H, et al. Xenon-enhanced CT CBF measurements in cerebral AVMs before and after excision. *J Neurosurg* **1983**;59:21–31
7. Takeuchi S, Kikuchi H, Karasawa J, et al. Local cerebral blood flow mapping by SPECT of N-isopropyl-p-[^{123}I] iodoamphetamine in comparison with ^{81m}Kr image. *Neurol Med Chir (Tokyo)* **1986**;26:369–378
8. Nishiya M, Kikuchi H, Karasawa J, et al. Evaluation of single photon emission computed tomography in occlusive cerebral vascular disease. *Prog Comput Tomogr* **1983**;5:277–283
9. Takeuchi S, Kikuchi H, Karasawa J, et al. A study of ^{81m}Kr perfusion images before and after vascular reconstructive surgery in the posterior fossa by using single-photon emission computed tomography. *Prog Comput Tomogr* **1984**;6:675–681
10. Hayashida K, Nishimura T, Uehara T, Kozuka T. Studies on in vivo labeling rate of red blood cells with ^{99m}Tc-pertechnetate in radionuclide angiography. *Kaku Igaku* **1981**;18:495–501
11. Winchell HS, Baldwin RM, Lin TH. Development of I-123-labeled amines for brain studies: localization of I-123 iodophenylalkyl amines in rat brain. *J Nucl Med* **1980**;21:940–946
12. Winchell HS, Horst WD, Braun L, Oldendorf WH, Hattner R, Parker H. N-isopropyl-[^{123}I] p-iodoamphetamine: single-pass brain uptake and washout; binding to brain synaptosomes; and localization in dog and monkey brain. *J Nucl Med* **1980**;21:947–952
13. Kuhl DE, Barrio JR, Huang SC, et al. Quantifying local cerebral blood flow by N-isopropyl-p-[^{123}I] iodoamphetamine (IMP) tomography. *J Nucl Med* **1982**;23:196–203
14. Fazio F, Nardini M, Fieschi C, Forli C. Assessment of regional cerebral blood flow by continuous carotid infusion of krypton-81m. *J Nucl Med* **1977**;18:962–966
15. Schiffer J, Bibi C, Avidan D. Cerebral arteriovenous malformation: papilledema as a presenting sign. *Surg Neurol* **1984**;22:524–526
16. Feindel W, Yamamoto YL, Hodge CP. Red cerebral veins and the cerebral steal syndrome. Evidence from fluorescein angiography and microregional blood flow by radioisotopes during excision of an angioma. *J Neurosurg* **1971**;35:167–179
17. Oldendorf WH, Kitano M. The free passage of I^{131} antipyrine through brain as an indication of A-V shunting. *Neurology* **1964**;14:1078–1083
18. Spetzler RF, Wilson CB, Weinstein P, Mehdorn M, Townsend J, Telles D. Normal perfusion pressure breakthrough theory. *Clin Neurosurg* **1978**;25:651–672
19. Jones FD, Boone SC, Whaley RA. Intracranial hemorrhage following attempted embolization and removal of large arteriovenous malformations. *Surg Neurol* **1982**;18:278–283
20. Day AL, Friedman WA, Sypert GW, Mickle JP. Successful treatment of normal perfusion pressure breakthrough syndrome. *Neurosurgery* **1982**;11:625–630